

---

# Feedback Linearization Based Trajectory Planning for a Planar Two-Link Bipedal Walking Robot

---

BTP Stage-I Report

By  
Shreyas N Bhat

Under the Guidance of  
Prof. Vivek Sangwan



Department of Mechanical Engineering  
Indian Institute of Technology, Bombay  
November, 2018

# Contents

<b>1</b>	<b>Introduction</b>	<b>3</b>
<b>2</b>	<b>Dynamic Model</b>	<b>3</b>
<b>3</b>	<b>Problem Formulation</b>	<b>5</b>
3.1	Feedback Linearizability . . . . .	5
3.2	Trajectory Planning . . . . .	6
<b>4</b>	<b>Results</b>	<b>7</b>
4.1	Convergence at an Infeasible Point . . . . .	7
4.2	First Convergence Using 14 Fourier Terms . . . . .	8
4.3	Second Convergence: Adding Another Constraint . . . . .	10
4.4	Third Convergence with Lower Back Swing . . . . .	12
<b>5</b>	<b>Conclusions</b>	<b>14</b>

## List of Figures

1	The biped . . . . .	3
2	The phases . . . . .	3
3	The infeasible convergence . . . . .	8
4	$q_1$ and $q_2$ , first convergence . . . . .	8
5	$\dot{q}_1$ and $\dot{q}_2$ , first convergence . . . . .	9
6	$y$ and $\ddot{y}$ , first convergence . . . . .	9
7	Heel height and Normal reaction, first convergence . . . . .	9
8	$q_1$ and $q_2$ , second convergence . . . . .	10
9	$\dot{q}_1$ and $\dot{q}_2$ , second convergence . . . . .	10
10	$y$ and $\ddot{y}$ , second convergence . . . . .	11
11	Heel height and Normal reaction, second convergence . . . . .	11
12	$q_1$ and $q_2$ , third convergence . . . . .	12
13	$\dot{q}_1$ and $\dot{q}_2$ , third convergence . . . . .	12
14	$y$ and $\ddot{y}$ , third convergence . . . . .	13
15	Heel height and Normal reaction, third convergence . . . . .	13

# 1 Introduction

The goal of this study is to perform a solution space analysis for the biped trajectory planning method mentioned in [1]. As a first step, one such trajectory was generated during this phase of the study. The concept of feedback linearization was used to convert the highly complex and nonlinear problem into a relatively easy to solve linear differential equation. At this stage, a solution to the problem that minimizes the energy input was found and in that process, all the background code that is required for the continuation of the study was set up.

## 2 Dynamic Model

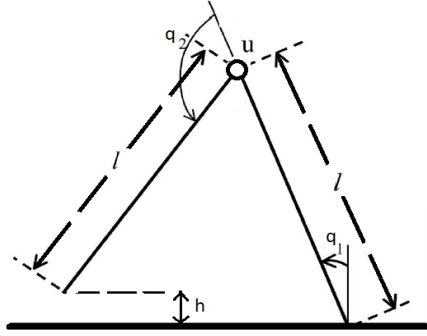


Figure 1: The biped consisting of two links connected at the hip with an actuator

The biped in this project consists of two links connected at the hip joint. It does not have any ankle joints, and hence, no feet. As a result, the system is underactuated when in the swing phase, that is, when one leg is firm on the ground and the other one is swinging to take a step. The mass distribution is such that the centre of mass of each link lies on the hip joint. This can be achieved by placing counterbalancing masses on the other side of the hip joint. This mass distribution helps in the formulation of the feedback linearization of the problem and also to make sure that the planned trajectories are dynamically feasible. The angles are defined as [1]. The stance leg angle  $q_1$  is defined with respect to the vertical while the angle  $q_2$  is defined with respect to the stance leg link. The actuator is placed at the hip joint. No actuator can be placed between the foot and the ground, hence leading to the underactuation in the biped.

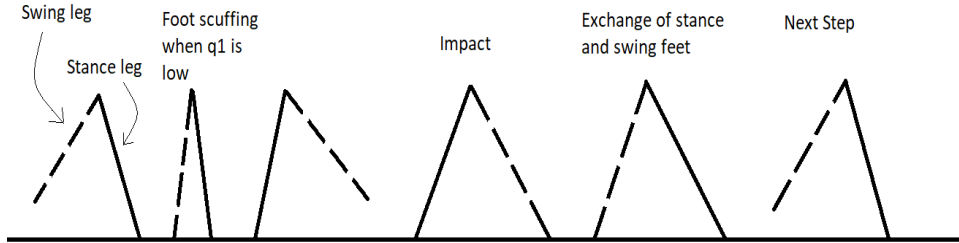


Figure 2: A step is shown with the phases that it is divided into. The change in the definition of angles post impact is apparent from this figure

The gait of the two linked biped was divided into two phases. One is the swing phase, wherein one of the legs remains stationary on the ground without slipping, while the other swings about the hip joint. This is a process which is continuous in time. The other is the impact phase in which both the legs come in contact with the ground and an instantaneous impact occurs with the ground. This leads to changes in the definition of the joint angles, since the stance leg is now the swing leg and vice versa. The impulsive forces at the ends of the legs also result in the change of the angular velocities of the joints. The absolute orientation of the biped, however, remains the same, since the process being instantaneous, such a change would result in infinitely large forces and torques. The impact occurs when the heel height is zero, that is when the angles satisfy the relation

$$2q_1 + q_2 = \pi \quad (1)$$

The dynamic equations were derived using the standard Lagrangian method

$$L = T - V \quad (2)$$

Where  $L$  is the Lagrangian,  $T$  is the kinetic energy of the system and  $V$  is the potential energy of the system. The equations were found by equating the Lagrangian derivative to zero, i.e.

$$\frac{d}{dt} \left( \frac{\partial L}{\partial \dot{q}} \right) - \frac{\partial L}{\partial q} = (0, u)^T \quad (3)$$

Using this and rearranging the terms, the equations were found out to be:

$$\begin{bmatrix} 1 & \epsilon \\ \epsilon & \epsilon \end{bmatrix} \begin{bmatrix} \ddot{q}_1 \\ \ddot{q}_2 \end{bmatrix} = \begin{bmatrix} \sin(q_1) \\ u \end{bmatrix} \quad (4)$$

The above equations are non-dimensional. The dimensionless parameters are:

$$\epsilon = \frac{I}{2(I + ml^2)}; \tau = \frac{t}{\sqrt{\frac{I + ml^2}{mgl}}}; u = \frac{u_2}{2mgl} \quad (5)$$

Here,  $m$  is the mass of each leg,  $I$  is the moment of inertia of each leg about its COM,  $l$  is the leg length,  $g$  is the acceleration due to gravity and  $u_2$  is the torque applied by the hip joint actuator.

This equation can be represented as:

$$D(q)\ddot{q} + G(q) = B(q)u \quad (6)$$

The impact between the swing leg and the ground is modelled as an inelastic collision between two rigid bodies. It is assumed that there is no slipping between the ground and the stance leg and that the swing leg gets off the ground without any interaction.

Since the contact needs to be fully defined, the cartesian co-ordinates of the stance leg are taken as  $(z_1, z_2)$  and the position of tip of the swing leg is parametrized using this reference frame.

The equation including this point as a state variable can be written as:

$$D_e(q)\ddot{q}_e + G_e(q_e) = B_e(q_e)u + \delta F_{ext} \quad (7)$$

Where  $\delta F_{ext}$  is the vector of external impulsional forces at the contact point of the swing leg with the ground and  $q_e$  is the vector  $(q_1, q_2, z_1, z_2)^T$ .

As the actuator cannot provide impulsional forces, integrating (5) over the time of the impact leads to:

$$D_e(q)(\dot{q}_e^+ - \dot{q}_e^-) = F_{ext} \quad (8)$$

Where  $F_{ext}$  is the result of integrating the external contact impulses over the impact duration.  $\dot{q}_e^+$  is the velocity just after impact and  $\dot{q}_e^-$  is the velocity just before impact.

Let  $\gamma(q_e)$  denote the coordinates of the swing leg in the reference frame  $(z_1, z_2)$ . Then,

$$\gamma(q_e) = \begin{bmatrix} z_1 + l\sin(q_1) + l\sin(q_2) \\ z_2 + l\cos(q_1) + l\cos(q_2) \end{bmatrix} \quad (9)$$

Now, we define the Jacobian matrix  $E$  as:

$$E = \frac{\partial \gamma(q_e)}{\partial q_e} \quad (10)$$

$$E = \begin{bmatrix} l \cos(q_1) & l \cos(q_2) & 1 & 0 \\ -l \sin(q_1) & -l \sin(q_2) & 0 & 1 \end{bmatrix} \quad (11)$$

Hence, by definition,  $F_{ext}$  is given by:

$$F_{ext} = E^T * \begin{bmatrix} F_T \\ F_N \end{bmatrix} \quad (12)$$

Now, we have 6 unknowns, namely,  $q_e^+$ ,  $F_T$  and  $F_N$  and 4 equations (8). The post impact angles  $q_e$  are known since it is assumed that there is no change in orientation of the biped during impact

$$q_e^+ = q_e^- \quad (13)$$

In order to get two more equations to solve the system, we impose the condition that the swing leg does not slip or rebound when it hits the ground. Hence,

$$\frac{d\gamma(q_e)}{dt} = 0 \quad (14)$$

i.e.

$$\frac{\partial \gamma(q_e)}{\partial q_e} \dot{q}_e^+ = 0 \quad (15)$$

i.e.

$$E * \dot{q}_e^+ = 0 \quad (16)$$

Thus giving us the remaining two equations.

Upon solving this system of equations, we would get the post impact state velocities  $\dot{q}_e^+$  and the forces  $F_T$  and  $F_N$ . However, since the stance leg and the swing leg interchange their roles after impact, the definitions of the angles are changed (they are defined w.r.t the stance leg). Hence, relabeling of the angles found after solving the equations is necessary.

After doing the relabeling, rearranging the terms and using the non-dimensional parameter  $\epsilon$  discussed earlier, we get the following relations for the impact:

$$\begin{bmatrix} q_1^+ \\ q_2^+ \end{bmatrix} = \begin{bmatrix} -\pi \\ 2\pi \end{bmatrix} + \begin{bmatrix} 1 & 1 \\ 0 & -1 \end{bmatrix} \begin{bmatrix} q_1^- \\ q_2^- \end{bmatrix} \quad (17)$$

$$\begin{bmatrix} \dot{q}_1^+ \\ \dot{q}_2^+ \end{bmatrix} = \left\{ \begin{bmatrix} 1 & 1 \\ 0 & -1 \end{bmatrix} + \frac{1-2\epsilon}{1-\epsilon} \begin{bmatrix} 1 + \cos(q_2^-) & 1 \\ -1 - \cos(q_2^-) & -1 \end{bmatrix} \right\} \begin{bmatrix} \dot{q}_1^- \\ \dot{q}_2^- \end{bmatrix} \quad (18)$$

### 3 Problem Formulation

The aim of this study was to find the input  $u$  as a function of time which when applied at the actuator would lead to a dynamically feasible and cyclic trajectory. The equations governing the motion of the biped (2) are, however, highly non-linear in nature, rendering them very difficult to solve directly.

#### 3.1 Feedback Linearizability

According to [1], the dynamics of the biped used in this study can be described with a single linearizing output trajectory and its derivatives. Through such a trajectory  $y$  and a finite number of its derivatives, it is possible to algebraically calculate the states  $(q_1, q_2, \dot{q}_1, \dot{q}_2)$  and the input  $u$ . This linearizing output is given by:

$$y = q_1 + \epsilon q_2 \quad (19)$$

From the first equation in (2), we know that  $\ddot{q}_1 + \epsilon\ddot{q}_2 = \sin(q_1)$  Hence,

$$\ddot{y} = \sin(q_1) \quad (20)$$

i.e.

$$q_1 = \sin^{-1}(\ddot{y}) \quad (21)$$

Using (19) and (21), we can derive the following relations:

$$q_2 = \frac{1}{\epsilon}(y - \sin^{-1}(\ddot{y})) \quad (22)$$

$$\dot{q}_1 = \frac{\ddot{y}}{\sqrt{1 - \ddot{y}^2}} \quad (23)$$

$$\dot{q}_2 = \frac{1}{\epsilon} \left( \dot{y} - \frac{\ddot{y}}{\sqrt{1 - \ddot{y}^2}} \right) \quad (24)$$

In this way, all the states can be represented algebraically through the linearizing output and its derivatives. To show that the input  $u$  can also be represented in the same way, we look at the second equation of (2), i.e.

$$\epsilon(\ddot{q}_1 + \ddot{q}_2) = u$$

Replacing the values of  $\ddot{q}_1$  and  $\ddot{q}_2$  with the time derivatives of (23) and (24), we get:

$$u = \ddot{y} - \frac{1 - \epsilon}{\sqrt{1 - \ddot{y}^2}} \left( y^{(4)} + \frac{\ddot{y}^2 \ddot{y}}{1 - \ddot{y}^2} \right) \quad (25)$$

Thus, by choosing a trajectory for  $y$ , we can compute the states and the input required to achieve this trajectory, making the system inherently dynamically feasible.

Also, for a feasible trajectory, we need to impose constraints on the Heel Height and the Normal Reaction offered by the ground. Hence, the equations for those were also derived and are presented below:

$$\frac{N}{2mg} = 1 - (1 - 2\epsilon)(\cos(q_1)\dot{q}_1^2 + \sin(q_1))\ddot{q}_1 \quad (26)$$

$$\frac{h}{l} = \cos(q_1) + \cos(q_1 + q_2) \quad (27)$$

Since the normal reaction offered by the ground is unidirectional (it cannot pull the leg towards it), the normal reaction term should always be  $\geq 0$ . The heel height of the swing leg must also be  $\geq 0$  since the tip of the swing leg should always be on or above the ground.

Thus, the problem that remained was to find a suitable trajectory in the linearizing output space, which passes through some predetermined points while satisfying the constraints. Hence, it was decided to pose this problem as an optimization problem.

### 3.2 Trajectory Planning

A suitable pre-impact state was chosen and the post impact state was calculated using the impact model. An intermediate state in the step (during foot scuffing) was also chosen. The time instant of the intermediate step and the step duration were also chosen. The corresponding linearizing output values were calculated using the relations (21)-(24). To find an initial trajectory, we fit a polynomial for the linearizing output trajectory such that it passes through these points.

The points that were chosen initially were,

$$q^- = (-\pi/9, -0.4, 11\pi/9, 0.2)^T \quad (28)$$

$$q_m = (-\pi/36, -0.12, 17\pi/18, 0.15)^T \quad (29)$$

The points were chosen such that at both the points (1) was satisfied, since at these points, both the feet touched the ground.

The time period of one step was chosen to be 2 seconds and the instant  $t_m$  at which the state  $q_m$  is achieved was taken as 1 second. The value of  $\epsilon$  was taken to be 0.07. The post-impact state was calculated by applying the impact model on  $q^-$ . A 11<sup>th</sup> degree polynomial  $y_1(t)$  was fit to pass through the points calculated from these values by using (21)-(24). In order for the states to be real,  $\ddot{y}$  should satisfy

$$|\ddot{y}| \leq 1 \quad (30)$$

This is necessary for (21) to be real. For meeting this constraint, an optimization problem was formulated. The final linearizing output trajectory was formulated as:

$$y = y_1(t) + t^4(t - t_m)^4(t - T)^4 F_s(t) \quad (31)$$

Where  $F_s(t)$  is a Fourier series given by:

$$F_s(t) = \sum_{k=0}^n \left( a_k \cos\left(\frac{2k\pi t}{T}\right) + b_k \sin\left(\frac{2k\pi t}{T}\right) \right) \quad (32)$$

The variables of optimization were the Fourier series coefficients  $a_k$  and  $b_k$ , the step time period  $T$ , the initial state  $q^-$ , the intermediate state  $q_m$  and the time instant of the intermediate step  $t_m$

The objective function to be minimized was:

$$f = u^T u \quad (33)$$

The constraints to be satisfied were the following:

$$T \leq T_{max} \quad (34)$$

$$-\pi/4 \leq q_1^- \leq 0 \quad (35)$$

$$N > 0 \quad (36)$$

$$h > 0 \quad (37)$$

$$\dot{q}_1 < 0 \quad (38)$$

$$-0.08 < q_{m1} < 0.08 \quad (39)$$

$$|\ddot{y}| \leq 1 \quad (40)$$

The first constraint was to ensure that the step period does not blow up to very large values. The second constraint was to ensure that the impact happens at a human-like posture, with the legs nor too close and neither too far from each other. The third and fourth constraints were discussed earlier. The fourth constraint ensures that the biped only moves in the forward direction. The fifth constraint is a reasonable assumption for the start of foot scuffing. The last constraint was also discussed earlier.

It was decided to concentrate on the most important constraint first, i.e. (40). The other constraints were not explicitly imposed on the model initially because our aim, at first, was to find one trajectory in the linearizing output space which could be used to calculate real outputs.

During each iteration, the values of the initial conditions provided was changed and hence, a different polynomial was fit in every iteration of the optimizer.

Details on the constraints applied and the corresponding results that were found are mentioned in sections below.

## 4 Results

### 4.1 Convergence at an Infeasible Point

During this go of the optimizing routine, we imposed the constraints (34),(35) and (40). 10 Fourier terms were used (5 sines and 5 cosines). It seems like this number was too less for the optimizer to converge at a feasible point. The solution that it came up with was quite better than the original polynomial that was fed into the system. However,  $\ddot{y}$  went out of bounds for a finite time interval



during the step, as can be seen from the figure below. This was not acceptable and hence, it was decided to increase the number of terms in the Fourier series used. We believed this would be the way to go since the imposed constraint was satisfied for most of the duration of the step, indicating that the optimizer was doing its job and it could not get a better result with the limited number of variables of optimization that it had.

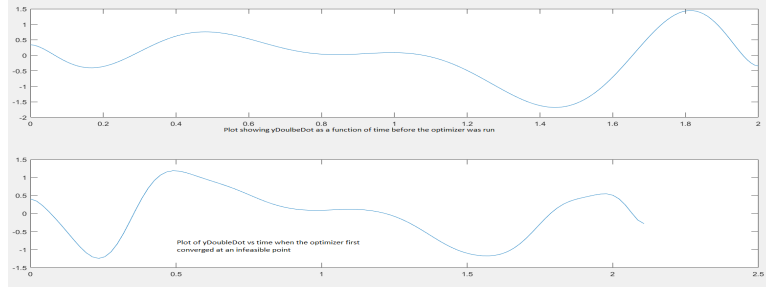


Figure 3: The optimizer had too few variables to work with and hence converged at an infeasible point.

## 4.2 First Convergence Using 14 Fourier Terms

The number of terms in the Fourier Series  $F_s$  was increased to 14. The optimizer did not converge but stopped due to reaching the maximum number of function computations thrice before actually converging at the solution. This was probably because the initial solution that we provided to the optimizer was significantly far from the final solution. But when it did converge, the optimizer came up with the initial conditions and the time interval for one step accordingly to satisfy this constraint. The solution, however, had some errors. The main error was that the swing leg was swinging wildly for a major part of the motion. The stance leg was also traveling backwards for some time, indicating that  $\dot{q}_1$  becomes positive for a while during the motion. This was undesirable, since we need the biped to continuously move forward. The plots provided below show the various quantities calculated using this first convergence.

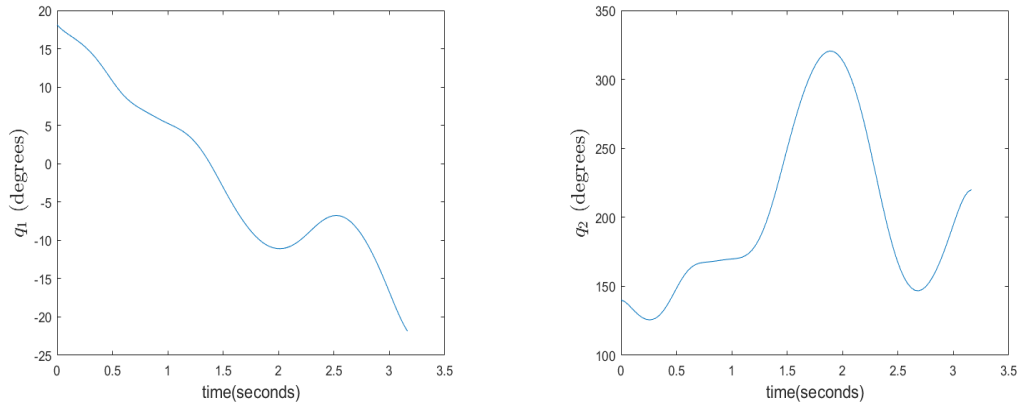


Figure 4: These figures show the variation of the joint angles  $q_1$  and  $q_2$  as a function of time for the first feasible convergence

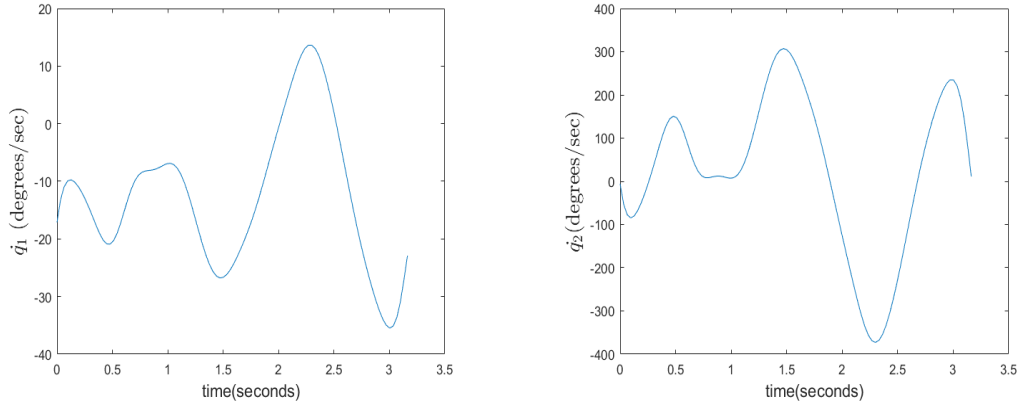


Figure 5: These figures show the variation in the joint angular velocities  $\dot{q}_1$  and  $\dot{q}_2$  with respect to time for the first feasible convergence

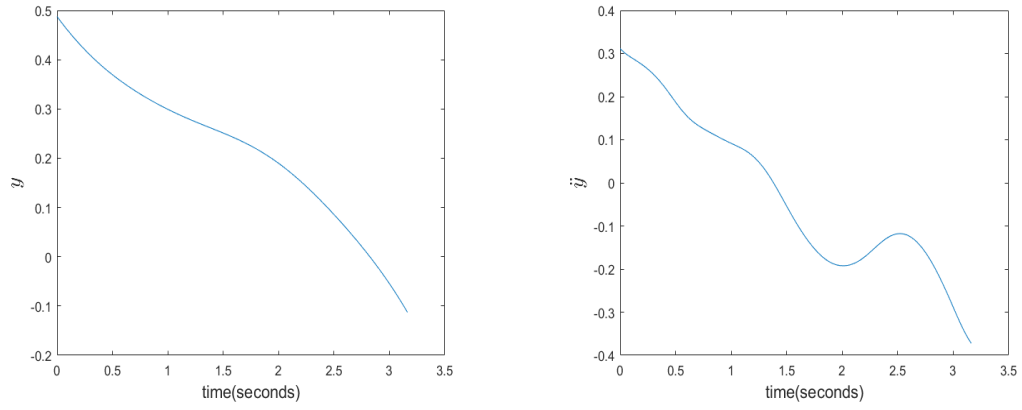


Figure 6: These figures show the variation in the the linearizing output trajectory and its second derivative with respect to time for the first feasible convergence

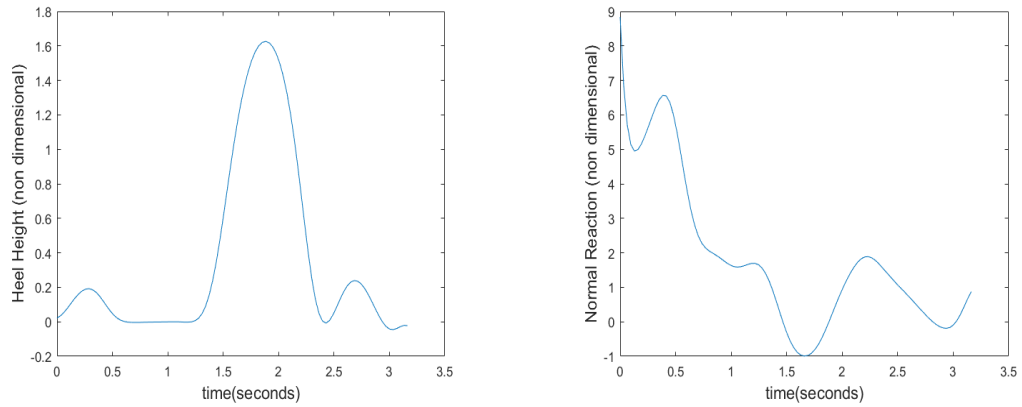


Figure 7: These figures show the variation in the the heel height and the normal reaction from the ground with respect to time for the first feasible convergence

### 4.3 Second Convergence: Adding Another Constraint

Once one solution was found, we proceeded to impose more constraints on the motion of the biped. We imposed (38) along with the constraints imposed earlier during this optimization routine. This constraint would ensure that the biped only moves forward. Using the values of the optimization variables found in the first convergence, it was possible to reach to this solution much faster. The resulting trajectory had a significant back swing of the swing leg during parts of the motion. The constraints had to be modified in order to decrease this swing back. However, the imposed constraints were satisfied for all the part of the motion.

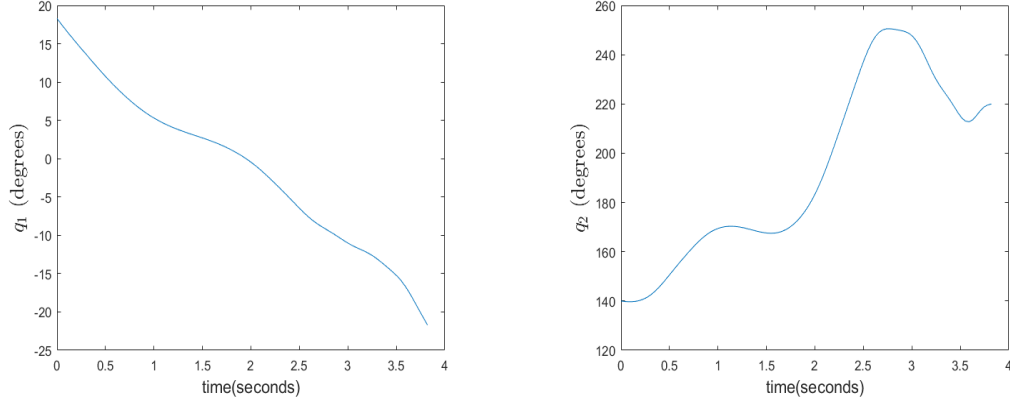


Figure 8: These figures show the variation of the joint angles  $q_1$  and  $q_2$  as a function of time for the second feasible convergence

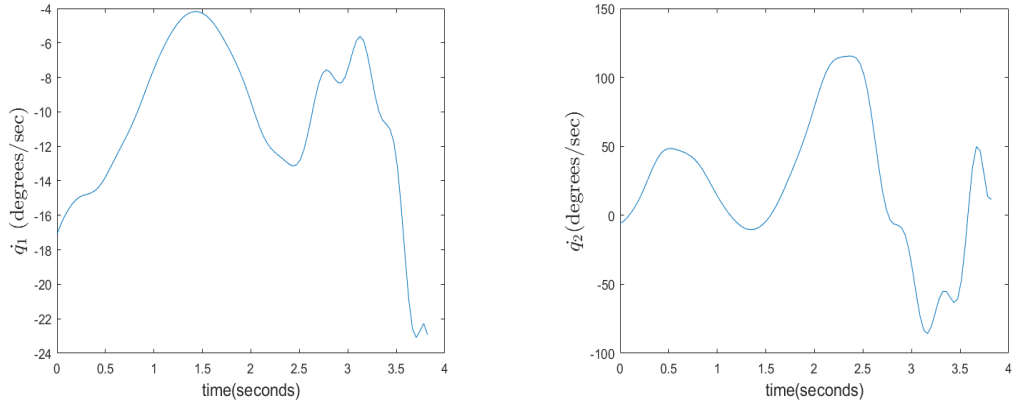


Figure 9: These figures show the variation in the joint angular velocities  $\dot{q}_1$  and  $\dot{q}_2$  with respect to time for the second feasible convergence

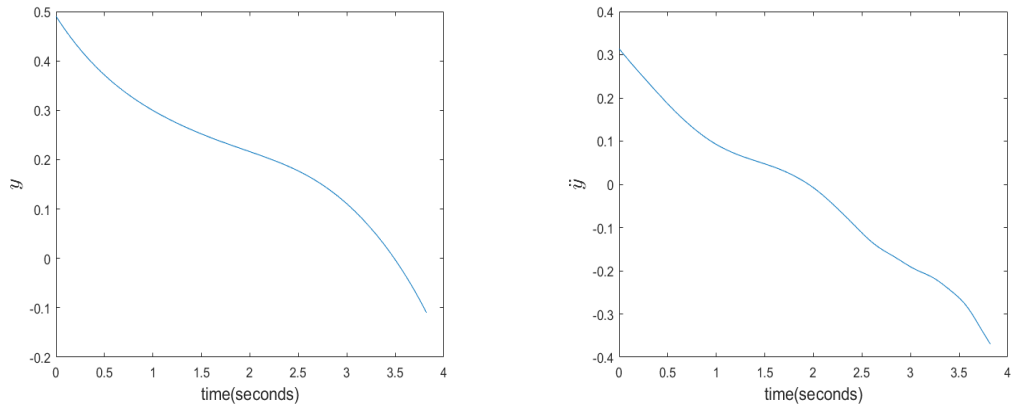


Figure 10: These figures show the variation in the the linearizing output trajectory and its second derivative with respect to time for the second feasible convergence

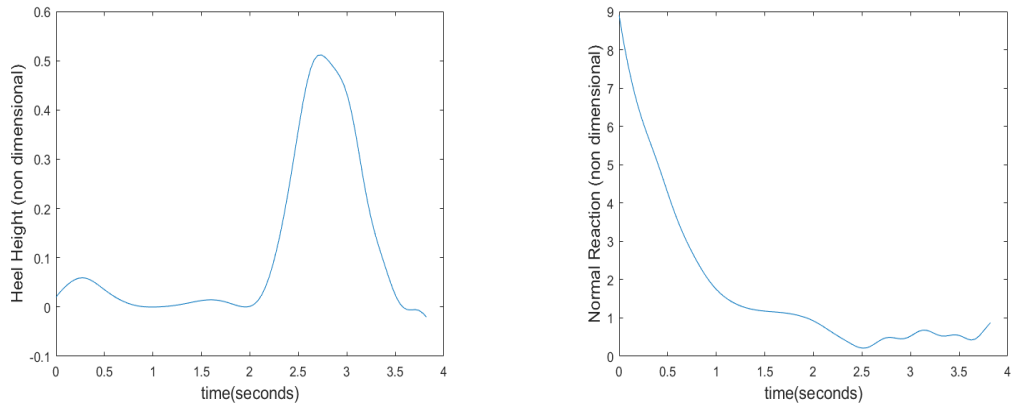


Figure 11: These figures show the variation in the the heel height and the normal reaction from the ground with respect to time for the second feasible convergence

#### 4.4 Third Convergence with Lower Back Swing

The second convergence had given us a solution that satisfied almost all the constraints throughout the duration of the step. The only problem that was present in that solution was the significant swing back of the swing leg during part of the motion, which was apparent from the animation. To reduce this swing back, I observed that  $q_2 - q_1$  was the angle of the swing leg from the vertical. For having a uniform forward motion of the swing leg, this angle should continue to decrease throughout the motion during a step. Hence, the next constraint imposed on the motion was:

$$\dot{q}_2 - \dot{q}_1 \leq 0 \quad (41)$$

The solution to this part, as expected, had significantly lower swing back of the leg throughout the step. This optimizer converged to this solution quite fast as well, since we already had the values for the optimization variables from the previous optimization routine. The figures below represent the various quantities calculated from this solution.

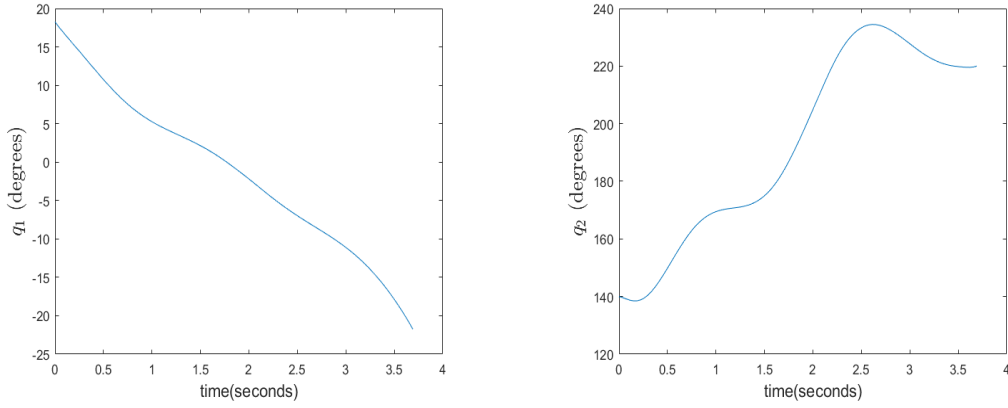


Figure 12: These figures show the variation of the joint angles  $q_1$  and  $q_2$  as a function of time for the third feasible convergence

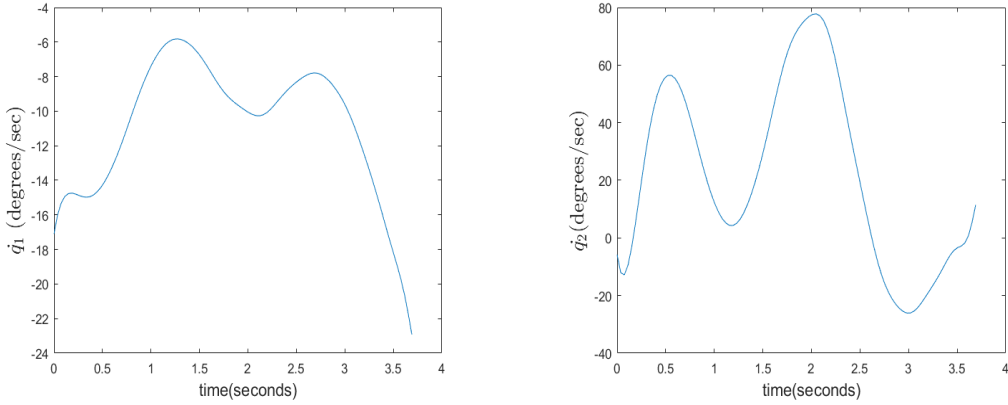


Figure 13: These figures show the variation in the joint angular velocities  $\dot{q}_1$  and  $\dot{q}_2$  with respect to time for the third feasible convergence

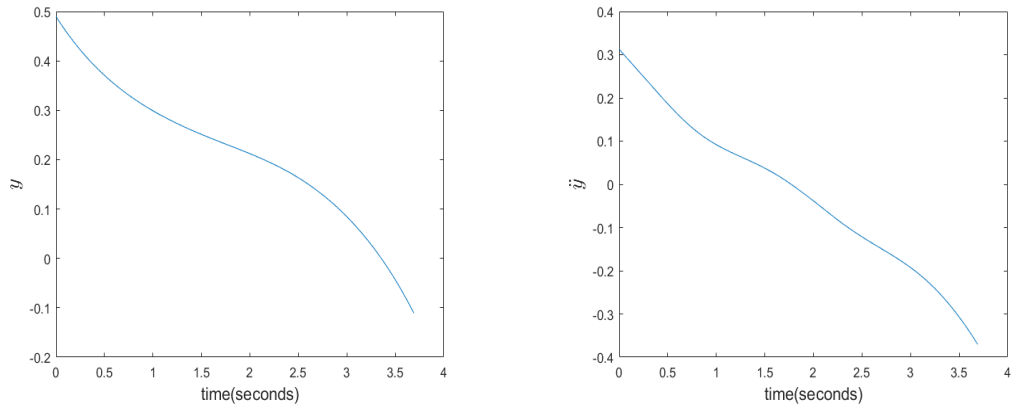


Figure 14: These figures show the variation in the the linearizing output trajectory and its second derivative with respect to time for the third feasible convergence

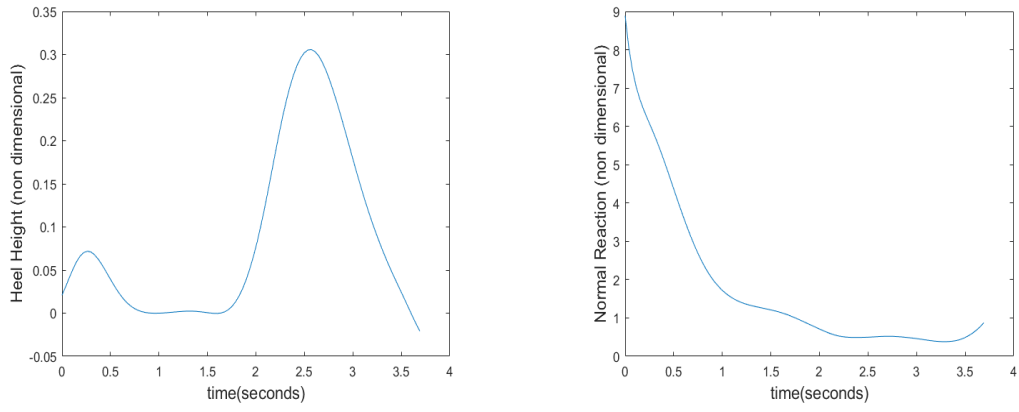


Figure 15: These figures show the variation in the the heel height and the normal reaction from the ground with respect to time for the third feasible convergence

## 5 Conclusions

The result of this initial study was that a dynamically feasible and cyclic solution to bipedal walking was found. Although it violated some constraints that were not explicitly imposed on the model, these constraints were violated on a very minor part of the whole trajectory, and hence it is believed that it should not be too difficult to ensure these constraints are met all the time. The background code has been set up for the continuation of this study, where it is the aim to find more such solutions by imposing different constraints and by using different initial conditions and objective functions.

## References

- [1] Vivek Sangwan and Sunil K. Agrawal. *Differentially Flat Design of Bipedal Ensuring Limit Cycles*. IEEE/ASME TRANSACTIONS ON MECHATRONICS, VOL. 14, NO. 6, DECEMBER 2009
- [2] Jesse W. Grizzle, Gabriel Abba, and Franck Plestan. *Asymptotically Stable Walking for Bipedal Robots: Analysis via Systems with Impulse Effects*. IEEE TRANSACTIONS ON AUTOMATIC CONTROL, VOL. 46, NO. 1, JANUARY 2001 51